



King Saud University

Arabian Journal of Chemistry

www.ksu.edu.sa
www.sciencedirect.com



ORIGINAL ARTICLE

Bounds on the partition dimension of one pentagonal carbon nancone structure



Ali N.A. Koam^a, Ali Ahmad^{b,*}, Muhammad Azeem^c, Muhammad Faisal Nadeem^d

^a Department of Mathematics, College of Science, Jazan University, New Campus, Jazan 2097, Saudi Arabia

^b College of Computer Science & Information Technology, Jazan University, Jazan, Saudi Arabia

^c Department of Mathematics, Riphah Institute of Computing and Applied Sciences, Riphah International University Lahore, Pakistan

^d Department of Mathematics, COMSATS University Islamabad, Lahore Campus, Lahore 54000, Pakistan

Received 14 December 2021; accepted 11 April 2022

Available online 22 April 2022

KEYWORDS

One pentagonal carbon nanocone;
Partition dimension;
Bounds on the partition dimension;
Resolving partition set

Abstract The partition dimension is the most complicated resolving parameter of all the resolvability parameters. In this parameter, the vertex set of a graph is completely subdivided into subsets so that each vertex of a graph has a unique identification in terms of the partitioning of its selected subsets. In this paper, we consider Carbon nanocone structure (CNC) more specifically one pentagonal carbon nanocone $CNC_{5,5}$. It is also regarded as a useful structure in terms of various applications. To delve deeper into this structure, we provide a graphical representation of it and identified sharp bounds for the partition dimension. We conclude that the pentagonal carbon nanocone $CNC_{5,5}$ has partition dimension ≤ 4 .

© 2022 The Author(s). Published by Elsevier B.V. on behalf of King Saud University. This is an open access article under the CC BY license (<http://creativecommons.org/licenses/by/4.0/>).

1. Introduction

The term metric dimension or in some literature employed as the metric index is widely studied in recent times due to the applicability in numerous fields, including chemistry of pharmaceuticals (Nadeem et al., 2020; Saenpholphat and Zhang, 2003), robot's navigation (Iijima and Ichihashi, 1993). Moreover, solar coast-Loran stations (Brinkmann and Cleemput,

2011), and in optimization employing combinatorics techniques (Johnson, 1993). When this concept is implemented in pharmaceuticals problems in drug design, mathematical representations for a set of chemical compounds are needed to find distinct representations for distinct compounds. A chemical compound structure can be modified into a labeled chemical network whose nodes and links are atoms and atom-bonds, respectively. The minimum number of nodes (atoms) provides the required distinct representations to distinct nodes (atoms) in the network due to the metric dimension concept (Chartrand et al., 2000).

Let $G = (V, E)$ be the connected graph. The distance between two vertices i, j of graph G is the length of the shortest path between them, and is usually denoted by $d(i, j)$. Let $S \subset V(G)$ the distance between $i \in V(G)$ and S is defined as $d(i, S) = \min\{d(i, k) : k \in S\}$. Let $R = \{r_1, r_2, \dots, r_n\}$ be an ordered set of $V(G)$. The metric codes of a vertex $i \in V(G)$ with

* Corresponding author.

E-mail addresses: akoum@jazanu.edu.sa (A.N.A. Koam), ahmadsms@gmail.com, aimam@jazanu.edu.sa (A. Ahmad).

Peer review under responsibility of King Saud University.



Production and hosting by Elsevier

respect to R is written as $r(i|R) = (d(i, r_1), d(i, r_2), \dots, d(i, r_n))$. The set R is usually known as resolving (distinguishing, determining) set of G if the metric codes of any two vertices of G are unique corresponding to R . The least number of elements within the distinguishing set of a graph G is called metric dimension, the usual notation in the literature is $\dim(G)$, (Slater, 1975).

Chemical graph theory aids interpretation of a chemical graph's nuclear assistant properties. Chemical graph theory is expected to play an important role in showcasing and organizing any constructed framework or component organize out. A chemical compound or graph is a graphical portrayal that includes atoms called vertices and atom-to-atom bonds known as edges.

Metric basis are very useful in the reshaping of a chemical network, therefore in the literature there is intensive research are available on different chemical structures, hollow coronoid structure is studied in this term (Mehreen et al., 2018), the necklace graph with these properties are discussed in (Khuller et al., 1996). The resolving set for the graph obtained from categorical product of two graphs available in (Arockiaraj et al., 2018), where a general circulant graphs are discussed in (Sebö and Tannier, 2004). Some of the results concerning metric dimension are detailed in (Estrada-Moreno, 2020; Liu et al., 2020; Valentini and Ciambella, 2016).

The concept of metric and partition dimension are closely related, as partition dimension is the generalization of the metric dimension. Instead of computing the distance between two vertices, we do it between a vertex and a set. The concept of partition dimension was introduced by (Chartrand et al., 2000).

Let $\sqcap = \{\sqcap_1, \sqcap_2, \dots, \sqcap_\ell\}$ be the partition of a connected graph. Now for a vertex $j \in V(G)$ the partition dimension with respect to \sqcap is $r(j|\sqcap) = (d(j, \sqcap_1), d(j, \sqcap_2), \dots, d(j, \sqcap_\ell))$, where $d(j, \sqcap_w) = \min\{d(j, y) : y \in \sqcap_w\}$ for $1 \leq w \leq \ell$. The distinct codes of the two vertices $i, j \in V(G)$ with respect to \sqcap , that is $r(i|\sqcap) \neq r(j|\sqcap)$, such a partition \sqcap is known as distinguishing partition of G (Koam and Ahmad, 2020; Alipour and Ashrafi, 2009).

Several authors have published articles related to the partition dimension of graphs; book graph are discussed in (Iijima, 1991) in terms of this concept, the resulted graph from the operation of comb product are detailed in (Ahmad and Sultan, 2017), generalized version of partition dimension are studied in (Imran et al., 2018; Ge and Sattler, 1994), and a generalized class of graphs are studied in terms of partition dimension in (Nadeem et al., 2021). The partition dimension for the families of circulant graphs, multipartite, and chemical graphs of fullerene are discussed in (Hussain et al., 2019; Baskoro and Haryeni, 2020). The graphs of convex polytopes for their partition dimension are in (Wei et al., 2021, 2021; Nadeem et al., 2021; Hussain et al., 2020). The graph with partition dimension $|V| - 3$ discussed (Akhter and Farooq, 2019).

The partition dimension, usually denoted as $pd(G)$, is the least number of elements residing in the distinguishing set \sqcap of G . In general for a connected graph G , we have.

$$pd(G) \leq \dim(G) + 1.$$

The emphasis of this study is finding the partition dimension problem of the 1-pentagonal carbon nanocone structure. In combinatorial chemistry, the set of atoms, molecules, and compounds are represented mathematically in a unique

manner for a large structure. The vertices and edges of a graph depict the atoms and bond types, respectively.

As mentioned, the partition dimension is the generalization of the metric dimension, so it would be interesting to find the partition dimension. This article was motivated by the results for the metric dimension of 1-pentagonal carbon nanocanes; this article found the partition dimension's sharps bounds.

2. 1-pentagonal carbon nanocone structure $CNC_{\zeta,5}$

Carbon nanocone (CNC) started its journey in 1994 (Amrullah et al., 2015), when it was treated in experimentation as 19° free standing cones, and it is found in the tunneling microscopy. It gained much attraction in the current era and came out in different topologies, such as carbon nanohorns (Vetrik and Ahmad, 2017; Bultheel and Ori, 2018). There is another construction of nanocone by putting a one-end cap on the nanotube (Cataldo et al., 2015; Iijima et al., 1992; Justus, 2007). Viewing oppositely, a nanocone with six pentagons contained an opening with 0° angle, which looks like a nanotube with one side of the face closed (capped). Moving towards one pentagonal nanocone observed or came into existence in the same year of 1994 (Amrullah et al., 2015). It is a proven statement that this particular type of nanocone is constructed from graphene structures. Removal of graphene is a 60° wedge, and after the joining of its edges formed a shape of a cone with a pentagonal defect on the side of the apex. For different study related to the carbon nanotubes, graphene sheets, and nanocones are available in (Azizkhani et al., 2020; Kolahchi and Kolahdouzan, 2021; Al-Furjan et al., 2020; Al-Furjan et al., 2021; Al-Furjan et al., 2021; Kolahchi et al., 2021; Faramoushjan et al., 2021).

It is widespread with its applicative point of view after discovering different types of nanocones and their topologies. The possible applications in energy storage, gas storage, gas sensors, biosensors, and chemical probes (Koam et al., 2021; Darmaji and Alfarsi, 2017; Maritz and Vetrik, 2017). Nanocones are carbon networks that can be represented as infinite cubic planar graphs. Authors in (Ahmad et al., 2018) investigated the topological modeling techniques of one pentagon carbon nanocones. Topological properties of carbon nanocones in (Ahmad et al., 2020), and computation calculation of wiener index in (Chu et al., 2020).

The Fig. 1 shows the molecular structure of nanocone, and it can be represented graphically by showing into vertices and edges form, which is in Fig. 2. As shown in Fig. 2 that the centermost cycle of with 5 vertices named as the first cycle, and the vertex set is defined as $V(CNC_{\zeta,5}) = \{\psi_{1,j} : 1 \leq j \leq 5\} \cup \{\psi_{2,j} : 1 \leq j \leq 15\} \cup \{\psi_{3,j} : 1 \leq j \leq 25\} \cup \{\psi_{4,j} : 1 \leq j \leq 35\} \cup \{\psi_{i,j} : 1 \leq i \leq \zeta, 1 \leq j \leq 10\epsilon - 5\} \cup \{\psi_{\zeta,j} : 1 \leq j \leq 10\epsilon - 5\}$.

The graph of $CNC_{\zeta}[n]$ comprises the conical structure possessing a cycle of length n and ζ layers of hexagons lying on the conical surface around its center. This article focuses primarily on the case when $n = 5$. The number of hexagons is represented as ζ incorporating the conical surface, and the number 5 indicates a pentagon lies on the tip known as the core. The metric dimension for $CNC_{\zeta,5}$ is obtained as;

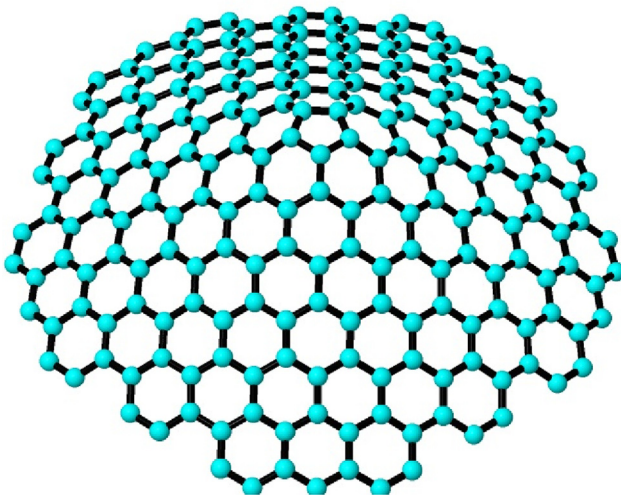


Fig. 1 Pentagonal Nanocone Structure.

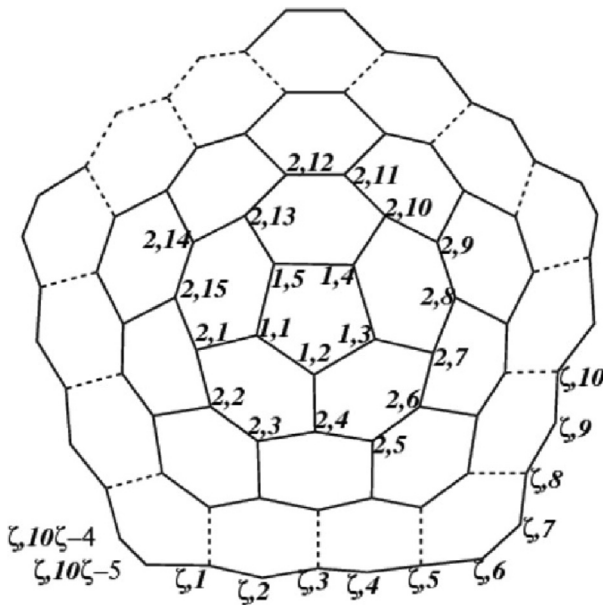


Fig. 2 One pentagonal nanocone: The labeling stated is the subscript or index of vertices. For example the 1, 1 is represented as $\psi_{1,1}$ in the results.

Theorem 2.1. [18] If $\zeta \geq 1$, then $\dim(CNC_{\zeta,5}) = 3$.

Now the following theorem is the sharp upper bounds on the partition dimension of one pentagonal nanocone structure $CNC_{\zeta,5}$. $CNC_{\zeta,5}$.

Theorem 2.2. Let $CNC_{\zeta,5}$ be a 1-pentagonal carbon nanocone structure with $\zeta \geq 1$. Then $pd(CNC_{\zeta,5}) \leq 4$.

Proof. To show that the partition dimension of $CNC_{\zeta,5}$ is ≤ 4 , suppose the resolving partition set $\sqcap = \{\sqcap_1, \sqcap_2, \sqcap_3, \sqcap_4\}$ where $\sqcap_1 = \{\psi_{\zeta,1}\}$, $\sqcap_2 = \{\psi_{\zeta,3}\}$, $\sqcap_3 = \{\psi_{\zeta,2\zeta+1}\}$, $\sqcap_4 = V(CNC_{\zeta,5}) \setminus \{\psi_{\zeta,1}, \psi_{\zeta,3}, \psi_{\zeta,2\zeta+1}\}$. The representations for the vertices of $CNC_{\zeta,5}$ are:

When $1 \leq j \leq 5$, the codes for the vertices with respect to the partition resolving set are following, in which the very first is the representations of the vertices of first and second cycle;

$$\begin{aligned} r(\psi_{1,1}|\sqcap) &= (2\zeta - 3, 2\zeta - 1, 2\zeta - 1, 0), \\ r(\psi_{1,2}|\sqcap) &= (2\zeta - 2, 2\zeta - 2, 2\zeta - 2, 0), \\ r(\psi_{1,3}|\sqcap) &= (2\zeta - 1, 2\zeta - 1, 2\zeta - 1, 0), r(\psi_{1,4}|\sqcap) \\ &= (2\zeta - 1, 2\zeta, 2\zeta, 0), \\ r(\psi_{1,5}|\sqcap) &= (2\zeta - 1, 2\zeta, 2\zeta, 0). \\ r(\psi_{2,1}|\sqcap) &= (2\zeta - 4, 2\zeta - 2, 2\zeta, 0), \\ r(\psi_{2,2}|\sqcap) &= (2\zeta - 5, 2\zeta - 3, 2\zeta - 1, 0), \\ r(\psi_{2,3}|\sqcap) &= (2\zeta - 4, 2\zeta - 4, 2\zeta - 2, 0), \\ r(\psi_{2,4}|\sqcap) &= (2\zeta - 3, 2\zeta - 3, 2\zeta - 3, 0), \\ r(\psi_{2,5}|\sqcap) &= (2\zeta - 2, 2\zeta - 2, 2\zeta - 4, 0), \\ r(\psi_{2,6}|\sqcap) &= (2\zeta - 1, 2\zeta - 1, 2\zeta - 3, 0), \\ r(\psi_{2,7}|\sqcap) &= (2\zeta, 2\zeta, 2\zeta - 2, 0), \\ r(\psi_{2,8}|\sqcap) &= (2\zeta + 1, 2\zeta + 1, 2\zeta - 1, 0), \\ r(\psi_{2,9}|\sqcap) &= (2\zeta + 1, 2\zeta + 2, 2\zeta, 0), \\ r(\psi_{2,10}|\sqcap) &= (2\zeta, 2\zeta + 1, 2\zeta + 1, 0), \\ r(\psi_{2,11}|\sqcap) &= (2\zeta + 1, 2\zeta + 2, 2\zeta + 2, 0), \\ r(\psi_{2,12}|\sqcap) &= (2\zeta, 2\zeta + 2, 2\zeta + 2, 0), \\ r(\psi_{2,13}|\sqcap) &= (2\zeta - 1, 2\zeta + 1, 2\zeta + 1, 0), \\ r(\psi_{2,14}|\sqcap) &= (2\zeta - 2, 2\zeta, 2\zeta + 2, 0), \\ r(\psi_{2,15}|\sqcap) &= (2\zeta - 3, 2\zeta - 1, 2\zeta + 1, 0). \end{aligned}$$

Representations of the vertices of third cycle;

$$\begin{aligned} r(\psi_{3,1}|\sqcap) &= (2\zeta - 6, 2\zeta - 4, 2\zeta - 1, 0), \\ r(\psi_{3,2}|\sqcap) &= (2\zeta - 7, 2\zeta - 5, 2\zeta - 1, 0), \\ r(\psi_{3,3}|\sqcap) &= (2\zeta - 6, 2\zeta - 6, 2\zeta - 2, 0), \\ r(\psi_{3,4}|\sqcap) &= (2\zeta - 5, 2\zeta - 5, 2\zeta - 3, 0), \\ r(\psi_{3,5}|\sqcap) &= (2\zeta - 4, 2\zeta - 4, 2\zeta - 4, 0), \\ r(\psi_{3,6}|\sqcap) &= (2\zeta - 3, 2\zeta - 3, 2\zeta - 5, 0), \\ r(\psi_{3,7}|\sqcap) &= (2\zeta - 2, 2\zeta - 2, 2\zeta - 6, 0), \\ r(\psi_{3,8}|\sqcap) &= (2\zeta - 1, 2\zeta - 1, 2\zeta - 5, 0), \\ r(\psi_{3,9}|\sqcap) &= (2\zeta, 2\zeta, 2\zeta - 4, 0), \\ r(\psi_{3,10}|\sqcap) &= (2\zeta + 1, 2\zeta + 1, 2\zeta - 3, 0), \\ r(\psi_{3,11}|\sqcap) &= (2\zeta + 2, 2\zeta + 2, 2\zeta - 2, 0), r(\psi_{3,12}|\sqcap) \\ &= (2\zeta + 3, 2\zeta + 3, 2\zeta - 1, 0), r(\psi_{3,13}|\sqcap) \\ &= (2\zeta + 3, 2\zeta + 4, 2\zeta - 1, 0), r(\psi_{3,14}|\sqcap) \\ &= (2\zeta + 2, 2\zeta + 3, 2\zeta + 1, 0), r(\psi_{3,15}|\sqcap) \\ &= (2\zeta + 3, 2\zeta + 4, 2\zeta + 4, 0), r(\psi_{3,16}|\sqcap) \\ &= (2\zeta + 2, 2\zeta + 3, 2\zeta + 3, 0), r(\psi_{3,17}|\sqcap) \\ &= (2\zeta + 3, 2\zeta + 4, 2\zeta + 4, 0), r(\psi_{3,18}|\sqcap) \\ &= (2\zeta + 2, 2\zeta + 4, 2\zeta + 4, 0), r(\psi_{3,19}|\sqcap) \\ &= (2\zeta + 1, 2\zeta + 3, 2\zeta + 3, 0), r(\psi_{3,20}|\sqcap) = (2\zeta, 2\zeta + 2, 2\zeta + 4, 0), \\ r(\psi_{3,21}|\sqcap) &= (2\zeta - 1, 2\zeta + 1, 2\zeta + 3, 0), r(\psi_{3,22}|\sqcap) = (2\zeta - 2, 2\zeta, 2\zeta + 4, 0), \\ r(\psi_{3,23}|\sqcap) &= (2\zeta - 3, 2\zeta - 1, 2\zeta + 3, 0), \\ r(\psi_{3,24}|\sqcap) &= (2\zeta - 4, 2\zeta - 2, 2\zeta + 2, 0), \\ r(\psi_{3,25}|\sqcap) &= (2\zeta - 5, 2\zeta - 3, 2\zeta + 1, 0). \end{aligned}$$

Representations of the vertices of fourth cycle are given in the [Tables 1 and 2](#).

Representations of the vertices of fifth cycle;

$$\begin{aligned} r(\psi_{5,1}|\sqcap) &= (2\zeta - 10, 2\zeta - 8, 2\zeta, 0), r(\psi_{5,2}|\sqcap) \\ &= (2\zeta - 11, 2\zeta - 9, 2\zeta - 1, 0), \end{aligned}$$

Table 1 Representations of the vertices of fourth cycle.

$r(. \Gamma)$	Γ_1	Γ_2	Γ_3	Γ_4	$r(. \Gamma)$	Γ_1	Γ_2	Γ_3	Γ_4
$\psi_{4,1}$	$2\zeta - 8$	$2\zeta - 6$	2ζ	0	$\psi_{4,3}$	$2\zeta - 8$	$2\zeta - 8$	$2\zeta - 2$	0
$\psi_{4,4}$	$2\zeta - 7$	$2\zeta - 7$	$2\zeta - 3$	0	$\psi_{4,5}$	$2\zeta - 6$	$2\zeta - 6$	$2\zeta - 4$	0
$\psi_{4,6}$	$2\zeta - 5$	$2\zeta - 5$	$2\zeta - 5$	0	$\psi_{4,7}$	$2\zeta - 4$	$2\zeta - 4$	$2\zeta - 6$	0
$\psi_{4,8}$	$2\zeta - 3$	$2\zeta - 3$	$2\zeta - 7$	0	$\psi_{4,9}$	$2\zeta - 2$	$2\zeta - 2$	$2\zeta - 8$	0
$\psi_{4,10}$	$2\zeta - 1$	$2\zeta - 1$	$2\zeta - 7$	0	$\psi_{4,11}$	2ζ	2ζ	$2\zeta - 6$	0
$\psi_{4,12}$	$2\zeta + 1$	$2\zeta + 1$	$2\zeta + 5$	0	$\psi_{4,13}$	$2\zeta + 2$	$2\zeta + 2$	$2\zeta + 4$	0
$\psi_{4,14}$	$2\zeta + 3$	$2\zeta + 3$	$2\zeta - 3$	0	$\psi_{4,15}$	$2\zeta + 4$	$2\zeta + 4$	$2\zeta + 2$	0

Table 2 Representations of the vertices of fourth cycle.

$r(. \Gamma)$	Γ_1	Γ_2	Γ_3	Γ_4	$r(. \Gamma)$	Γ_1	Γ_2	Γ_3	Γ_4
$\psi_{4,16}$	$2\zeta + 5$	$2\zeta + 5$	$2\zeta - 1$	0	$\psi_{4,17}$	$2\zeta + 5$	$2\zeta + 6$	2ζ	0
$\psi_{4,18}$	$2\zeta + 4$	$2\zeta + 5$	$2\zeta + 1$	0	$\psi_{4,19}$	$2\zeta + 5$	$2\zeta + 6$	$2\zeta + 2$	0
$\psi_{4,20}$	$2\zeta + 4$	$2\zeta + 5$	$2\zeta + 3$	0	$\psi_{4,21}$	$2\zeta + 5$	$2\zeta + 6$	$2\zeta + 4$	0
$\psi_{4,22}$	$2\zeta + 4$	$2\zeta + 5$	$2\zeta + 5$	0	$\psi_{4,23}$	$2\zeta + 5$	$2\zeta + 6$	$2\zeta + 6$	0
$\psi_{4,24}$	$2\zeta + 4$	$2\zeta + 6$	$2\zeta + 6$	0	$\psi_{4,25}$	$2\zeta + 3$	$2\zeta + 5$	$2\zeta + 5$	0
$\psi_{4,26}$	$2\zeta + 2$	$2\zeta + 4$	$2\zeta + 6$	0	$\psi_{4,27}$	$2\zeta + 1$	$2\zeta + 3$	$2\zeta + 5$	0
$\psi_{4,28}$	2ζ	$2\zeta + 2$	$2\zeta + 6$	0	$\psi_{4,29}$	$2\zeta - 1$	$2\zeta + 1$	$2\zeta + 5$	0
$\psi_{4,30}$	$2\zeta - 2$	2ζ	$2\zeta + 6$	0	$\psi_{4,31}$	$2\zeta - 3$	$2\zeta - 1$	$2\zeta + 5$	0
$\psi_{4,32}$	$2\zeta - 4$	$2\zeta - 2$	$2\zeta + 4$	0	$\psi_{4,33}$	$2\zeta - 5$	$2\zeta - 3$	$2\zeta + 3$	0
$\psi_{4,34}$	$2\zeta - 6$	$2\zeta - 4$	$2\zeta + 2$	0	$\psi_{4,35}$	$2\zeta - 7$	$2\zeta - 5$	$2\zeta + 1$	0

$$\begin{aligned}
 r(\psi_{5,3}|\Gamma) &= (2\zeta - 10, 2\zeta - 10, 2\zeta - 2, 0), \\
 r(\psi_{5,4}|\Gamma) &= (2\zeta - 9, 2\zeta - 9, 2\zeta - 3, 0), \\
 r(\psi_{5,5}|\Gamma) &= (2\zeta - 8, 2\zeta - 8, 2\zeta - 4, 0), \\
 r(\psi_{5,6}|\Gamma) &= (2\zeta - 7, 2\zeta - 7, 2\zeta - 5, 0), \\
 r(\psi_{5,7}|\Gamma) &= (2\zeta - 6, 2\zeta - 6, 2\zeta - 6, 0), r(\psi_{5,8}|\Gamma) \\
 &= (2\zeta - 5, 2\zeta - 5, 2\zeta - 7, 0), \\
 r(\psi_{5,9}|\Gamma) &= (2\zeta - 4, 2\zeta - 4, 2\zeta - 8, 0), \\
 r(\psi_{5,10}|\Gamma) &= (2\zeta - 3, 2\zeta - 3, 2\zeta - 9, 0), \\
 r(\psi_{5,11}|\Gamma) &= (2\zeta - 2, 2\zeta - 2, 2\zeta - 10, 0), r(\psi_{5,12}|\Gamma) \\
 &= (2\zeta - 1, 2\zeta - 1, 2\zeta - 9, 0), \\
 r(\psi_{5,13}|\Gamma) &= (2\zeta, 2\zeta, 2\zeta + 8, 0), \\
 r(\psi_{5,14}|\Gamma) &= (2\zeta + 1, 2\zeta + 1, 2\zeta - 7, 0), \\
 r(\psi_{5,15}|\Gamma) &= (2\zeta + 2, 2\zeta + 2, 2\zeta - 6, 0), r(\psi_{5,16}|\Gamma) \\
 &= (2\zeta + 3, 2\zeta + 3, 2\zeta - 5, 0), \\
 r(\psi_{5,17}|\Gamma) &= (2\zeta + 4, 2\zeta + 4, 2\zeta - 4, 0), r(\psi_{5,18}|\Gamma) \\
 &= (2\zeta + 5, 2\zeta + 5, 2\zeta - 3, 0), \\
 r(\psi_{5,19}|\Gamma) &= (2\zeta + 6, 2\zeta + 6, 2\zeta - 2, 0), r(\psi_{5,20}|\Gamma) \\
 &= (2\zeta + 7, 2\zeta + 7, 2\zeta - 1, 0), \\
 r(\psi_{5,21}|\Gamma) &= (2\zeta + 7, 2\zeta + 8, 2\zeta, 0), r(\psi_{5,22}|\Gamma) \\
 &= (2\zeta + 6, 2\zeta + 7, 2\zeta + 1, 0), \\
 r(\psi_{5,23}|\Gamma) &= (2\zeta + 7, 2\zeta + 8, 2\zeta + 2, 0), r(\psi_{5,24}|\Gamma) \\
 &= (2\zeta + 6, 2\zeta + 7, 2\zeta + 3, 0), \\
 r(\psi_{5,25}|\Gamma) &= (2\zeta + 7, 2\zeta + 8, 2\zeta + 4, 0), r(\psi_{5,26}|\Gamma) \\
 &= (2\zeta + 6, 2\zeta + 7, 2\zeta + 5, 0), \\
 r(\psi_{5,27}|\Gamma) &= (2\zeta + 7, 2\zeta + 8, 2\zeta + 6, 0), \\
 r(\psi_{5,28}|\Gamma) &= (2\zeta + 6, 2\zeta + 7, 2\zeta + 7, 0), \\
 r(\psi_{5,29}|\Gamma) &= (2\zeta + 7, 2\zeta + 8, 2\zeta + 8, 0), r(\psi_{5,30}|\Gamma) \\
 &= (2\zeta + 6, 2\zeta + 8, 2\zeta + 8, 0), \\
 r(\psi_{5,31}|\Gamma) &= (2\zeta + 5, 2\zeta + 7, 2\zeta + 7, 0), r(\psi_{5,32}|\Gamma) \\
 &= (2\zeta + 4, 2\zeta + 6, 2\zeta + 8, 0),
 \end{aligned}$$

$$\begin{aligned}
 r(\psi_{5,33}|\Gamma) &= (2\zeta + 3, 2\zeta + 5, 2\zeta + 7, 0), r(\psi_{5,34}|\Gamma) \\
 &= (2\zeta + 2, 2\zeta + 4, 2\zeta + 8, 0), \\
 r(\psi_{5,35}|\Gamma) &= (2\zeta + 1, 2\zeta + 3, 2\zeta + 2, 0), r(\psi_{5,36}|\Gamma) \\
 &= (2\zeta, 2\zeta + 2, 2\zeta + 8, 0), \\
 r(\psi_{5,37}|\Gamma) &= (2\zeta - 1, 2\zeta + 1, 2\zeta + 7, 0), r(\psi_{5,38}|\Gamma) \\
 &= (2\zeta - 2, 2\zeta, 2\zeta + 8, 0), \\
 r(\psi_{5,39}|\Gamma) &= (2\zeta - 3, 2\zeta - 1, 2\zeta + 7, 0), r(\psi_{5,40}|\Gamma) \\
 &= (2\zeta - 4, 2\zeta - 2, 2\zeta + 6, 0), \\
 r(\psi_{5,41}|\Gamma) &= (2\zeta - 5, 2\zeta - 3, 2\zeta + 5, 0), r(\psi_{5,42}|\Gamma) \\
 &= (2\zeta + 6, 2\zeta - 4, 2\zeta + 4, 0), \\
 r(\psi_{5,43}|\Gamma) &= (2\zeta - 7, 2\zeta - 5, 2\zeta + 3, 0), \\
 r(\psi_{5,44}|\Gamma) &= (2\zeta - 8, 2\zeta - 6, 2\zeta + 2, 0), \\
 r(\psi_{5,45}|\Gamma) &= (2\zeta - 9, 2\zeta - 7, 2\zeta + 1, 0).
 \end{aligned}$$

So the generalize set of vertices representations are given in the **Table 3** and onward;

$$\begin{aligned}
 &\text{Representations of the vertices with } 6 \leq \epsilon \leq \zeta - 1; \\
 r(\psi_{\epsilon,2\epsilon+1}|\Gamma) &= (2\zeta - 2, 2\zeta - 2, 2\zeta - 2\epsilon, 0), \\
 r(\psi_{\epsilon,2\epsilon+2}|\Gamma) &= (2\zeta - 1, 2\zeta - 1, 2\zeta - 2\epsilon + 1, 0), \\
 r(\psi_{\epsilon,2\epsilon+3}|\Gamma) &= (2\zeta, 2\zeta, 2\zeta - 2\epsilon + 3, 0), \\
 r(\psi_{\epsilon,2\epsilon+4}|\Gamma) &= (2\zeta + 1, 2\zeta + 1, 2\zeta - 2\epsilon + 3, 0), \\
 r(\psi_{\epsilon,2\epsilon+5}|\Gamma) &= (2\zeta + 2, 2\zeta + 2, 2\zeta - 2\epsilon + 4, 0), \\
 r(\psi_{\epsilon,4\epsilon}|\Gamma) &= (2\zeta - 3 + 2\epsilon, 2\zeta - 3 + 2\epsilon, 2\zeta - 1, 0), \\
 r(\psi_{\epsilon,4\epsilon+1}|\Gamma) &= (2\zeta - 3 + 2\epsilon, 2\zeta - 2 + 2\epsilon, 2\zeta, 0), \\
 r(\psi_{\epsilon,4\epsilon+2}|\Gamma) &= (2\zeta - 4 + 2\epsilon, 2\zeta - 3 + 2\epsilon, 2\zeta + 1, 0), \\
 r(\psi_{\epsilon,4\epsilon+3}|\Gamma) &= (2\zeta - 3 + 2\epsilon, 2\zeta - 2 + 2\epsilon, 2\zeta + 2, 0), \\
 r(\psi_{\epsilon,6\epsilon-1}|\Gamma) &= (2\zeta - 3 + 2\epsilon, 2\zeta - 2 + 2\epsilon, 2\zeta - 2 + 2\epsilon, 0), \\
 r(\psi_{\epsilon,6\epsilon}|\Gamma) &= (2\zeta - 4 + 2\epsilon, 2\zeta - 2 + 2\epsilon, 2\zeta - 2 + 2\epsilon, 0), \\
 r(\psi_{\epsilon,6\epsilon+1}|\Gamma) &= (2\zeta - 5 + 2\epsilon, 2\zeta - 3 + 2\epsilon, 2\zeta - 3 + 2\epsilon, 0), \\
 r(\psi_{\epsilon,6\epsilon+2}|\Gamma) &= (2\zeta - 6 + 2\epsilon, 2\zeta - 4 + 2\epsilon, 2\zeta - 2 + 2\epsilon, 0),
 \end{aligned}$$

Table 3 Representations of the vertices with $6 \leq \epsilon \leq \zeta - 1$.

$r(\psi_{\epsilon,1} \sqcap)$	$(2\zeta - 2\epsilon, 2\zeta - 2\epsilon + 2, 2\zeta, 0)$
$r(\psi_{\epsilon,2} \sqcap)$	$(2\zeta - 2\epsilon - 1, 2\zeta - 2\epsilon + 1, 2\zeta - 1, 0)$
$r(\psi_{\epsilon,3} \sqcap)$	$(2\zeta - 2\epsilon, 2\zeta - 2\epsilon, 2\zeta - 2, 0)$
$r(\psi_{\epsilon,4} \sqcap)$	$(2\zeta - 2\epsilon + 1, 2\zeta - 2\epsilon + 1, 2\zeta - 3, 0)$
$r(\psi_{\epsilon,5} \sqcap)$	$(2\zeta - 2\epsilon + 2, 2\zeta - 2\epsilon + 2, 2\zeta - 4, 0)$
$r(\psi_{\epsilon,6} \sqcap)$	$(2\zeta - 2\epsilon + 3, 2\zeta - 2\epsilon + 3, 2\zeta - 5, 0)$
$r(\psi_{\epsilon,7} \sqcap)$	$(2\zeta - 2\epsilon + 4, 2\zeta - 2\epsilon + 4, 2\zeta - 6, 0)$
$r(\psi_{\epsilon,8} \sqcap)$	$(2\zeta - 2\epsilon + 5, 2\zeta - 2\epsilon + 5, 2\zeta - 7, 0)$
$r(\psi_{\epsilon,9} \sqcap)$	$(2\zeta - 2\epsilon + 6, 2\zeta - 2\epsilon + 6, 2\zeta - 8, 0)$
$r(\psi_{\epsilon,10} \sqcap)$	$(2\zeta - 2\epsilon + 7, 2\zeta - 2\epsilon + 7, 2\zeta - 9, 0)$
$r(\psi_{\epsilon,11} \sqcap)$	$(2\zeta - 2\epsilon + 8, 2\zeta - 2\epsilon + 8, 2\zeta - 10, 0)$

$$\begin{aligned} r(\psi_{\epsilon,6\epsilon+3}|\sqcap) &= (2\zeta - 7 + 2\epsilon, 2\zeta - 5 + 2\epsilon, 2\zeta - 3 + 2\epsilon, 0), \\ r(\psi_{\epsilon,8\epsilon-1}|\sqcap) &= (2\zeta - 3, 2\zeta - 1, 2\zeta - 3 + 2\epsilon, 0), \\ r(\psi_{\epsilon,8\epsilon}|\sqcap) &= (2\zeta - 4, 2\zeta - 2, 2\zeta - 4 + 2\epsilon, 0), \\ r(\psi_{\epsilon,8\epsilon+1}|\sqcap) &= (2\zeta - 5, 2\zeta - 3, 2\zeta - 5 + 2\epsilon, 0), \\ r(\psi_{\epsilon,10\epsilon-5}|\sqcap) &= (2\zeta + 1 - 2\epsilon, 2\zeta + 3 - 2\epsilon, 2\zeta + 1, 0). \end{aligned}$$

For the vertices on the ζ^{th} cycle representations are;

$$\begin{aligned} r(\psi_{\zeta,1}|\sqcap) &= (0, 2, 2\zeta, 1), r(\psi_{\zeta,2}|\sqcap) = (1, 1, 2\zeta - 1, 0), \\ r(\psi_{\zeta,3}|\sqcap) &= (2, 0, 2\zeta - 2, 1), r(\psi_{\zeta,4}|\sqcap) = (3, 1, 2\zeta - 3, 0), \\ r(\psi_{\zeta,2\zeta}|\sqcap) &= (2\zeta - 1, 2\zeta - 3, 1, 0), \\ r(\psi_{\zeta,2\zeta+1}|\sqcap) &= (2\zeta, 2\zeta - 2, 0, 1), \\ r(\psi_{\zeta,2\zeta+3}|\sqcap) &= (2\zeta, 2\zeta, 2, 0), \\ r(\psi_{\zeta,2\zeta+4}|\sqcap) &= (2\zeta + 1, 2\zeta + 1, 3, 0), \\ r(\psi_{\zeta,2\zeta+5}|\sqcap) &= (2\zeta + 2, 2\zeta + 2, 4, 0), \\ r(\psi_{\zeta,4\zeta}|\sqcap) &= (4\zeta - 3, 4\zeta - 3, 2\zeta - 1, 0), \\ r(\psi_{\zeta,4\zeta+1}|\sqcap) &= (4\zeta, 4\zeta, 2\zeta, 0), \\ r(\psi_{\zeta,4\zeta+2}|\sqcap) &= (4\zeta - 3, 4\zeta - 3, 2\zeta + 1, 0), \\ r(\psi_{\zeta,4\zeta+3}|\sqcap) &= (4\zeta - 3, 4\zeta - 2, 2\zeta + 2, 0), \\ r(\psi_{\zeta,4\zeta+4}|\sqcap) &= (4\zeta - 4, 4\zeta - 3, 2\zeta + 3, 0), \\ r(\psi_{\zeta,4\zeta+5}|\sqcap) &= (4\zeta - 3, 4\zeta - 2, 2\zeta + 4, 0). \end{aligned}$$

Representations of the vertices on outer cycle;

$$\begin{aligned} r(\psi_{\zeta,6\zeta-1}|\sqcap) &= (4\zeta - 3, 4\zeta - 2, 4\zeta - 2, 0), \\ r(\psi_{\zeta,6\zeta}|\sqcap) &= (4\zeta - 4, 4\zeta - 2, 4\zeta - 2, 0), \\ r(\psi_{\zeta,6\zeta+1}|\sqcap) &= (4\zeta - 5, 4\zeta - 3, 4\zeta - 3, 0), \\ r(\psi_{\zeta,6\zeta+2}|\sqcap) &= (4\zeta - 6, 4\zeta - 4, 4\zeta - 2, 0), \\ r(\psi_{\zeta,7\zeta-1}|\sqcap) &= (3\zeta - 3, 3\zeta - 1, 4\zeta - 2, 0), \\ r(\psi_{\zeta,7\zeta}|\sqcap) &= (3\zeta - 4, 3\zeta - 2, 4\zeta - 3, 0), \\ r(\psi_{\zeta,7\zeta+1}|\sqcap) &= (3\zeta - 5, 3\zeta - 3, 4\zeta - 2, 0), \\ r(\psi_{\zeta,7\zeta+2}|\sqcap) &= (3\zeta - 6, 3\zeta - 4, 4\zeta - 3, 0), \\ r(\psi_{\zeta,8\zeta}|\sqcap) &= (2\zeta - 4, 2\zeta - 2, 4\zeta - 4, 0), \\ r(\psi_{\zeta,8\zeta+1}|\sqcap) &= (2\zeta - 5, 2\zeta - 3, 4\zeta - 5, 0), \\ r(\psi_{\zeta,8\zeta+2}|\sqcap) &= (2\zeta - 6, 2\zeta - 4, 4\zeta - 6, 0), \\ r(\psi_{\zeta,10\zeta-6}|\sqcap) &= (2, 4, 2\zeta + 2, 0), \\ r(\psi_{\zeta,10\zeta-5}|\sqcap) &= (1, 3, 2\zeta + 1, 0). \end{aligned}$$

From these representations given above, one can see that all the vertices of $CNC_{\zeta,5}$ have distinct representations with respect to \sqcap . Thus \sqcap is resolving partitioning for $CNC_{\zeta,5}$. Hence, for all $\zeta \geq 1$,

$$pd(CNC_{\zeta,5}) \leq 4.$$

3. Conclusion

Carbon nanocone structure (CNC) and more specifically one pentagonal carbon nanocone $CNC_{\zeta,5}$ is the energy and gas storage devices. It also considered as beneficial structure in terms of different applications. To dive deep into this structure we provide a graphical plot of this emerged structure and found out a resolving parameter which is known as the partition dimension. In this parameter a graph or structure's vertex set wholly subdivide into subsets such that each vertex of a graph have unique identification in terms of its selected subsets partitioning. We conclude that the pentagonal carbon nanocone $CNC_{\zeta,5}$ has partition dimension ≤ 4 .

4. Availability of data and material

There is not data associated with this manuscript.

Funding

There is not funding associated with this manuscript.

Declaration of Competing Interest

The authors declare that they have no known competing financial interests or personal relationships that could have appeared to influence the work reported in this paper.

Acknowledgements

N/A

References

- Ahmad, A., Bača, M., Sultan, S., 2020. Computing the metric dimension of Kayak Paddles graph and Cycles with chord. *Proyecciones J. Math.* 39 (2), 287–300.
- Ahmad, A., Baca, M., Sultan, S., 2018. Minimal doubly resolving sets of Necklace graph. *Math. Rep.* 20 (70) (2), 123–129.
- Ahmad, A., Sultan, S., 2017. On minimal doubly resolving sets of circulant graphs. *Acta Mech. Slovaca* 20 (1), 6–11.
- Akhter, S., Farooq, R., 2019. Metric dimension of fullerene graphs. *Electron. J. Graph Theory* 7 (1), 91–103.
- Al-Furjan, M.S.H., Farrokhan, A., Keshtegar, B., Kolahchi, R., Trung, N.-T., 2020. Higher order nonlocal viscoelastic strain gradient theory for dynamic buckling analysis of carbon nanocones. *Aerosp. Sci. Technol.* 107,. <https://doi.org/10.1016/j.ast.2020.106259> 106259.
- Al-Furjan, M.S.H., Farrokhan, A., Mahmoud, S.R., Kolahchi, R., 2021. Dynamic deflection and contact force histories of graphene platelets reinforced conical shell integrated with magnetostrictive layers subjected to low-velocity impact. *Thin-Walled Struct.* 163,. <https://doi.org/10.1016/j.tws.2021.107706> 107706.
- Al-Furjan, M.S.H., Farrokhan, A., Keshtegar, B., Kolahchi, R., Trung, N.-T., 2021. Dynamic stability control of viscoelastic nanocomposite piezoelectric sandwich beams resting on Kerr foundation based on exponential piezoelasticity theory. *Eur. J. Mech. A. Solids* 86,. <https://doi.org/10.1016/j.euromechsol.2020.104169> 104169.
- Alipour, M.A., Ashrafi, A.R., 2009. Computer calculation of the wiener index of one-pentagonal carbon nanocone. *Digest J. Nanomater. Biostruct.* 4 (1).

- Amrullah, E.T., Baskoro, R.S., Uttungadewa, S., 2015. The partition dimension of a subdivision of a complete graph. *Procedia Comput. Sci.* 74, 53–59.
- Arockiaraj, M., Clement, J., Balasubramanian, K., 2018. Topological properties of carbon nanocones. *Polycyclic Aromat. Compd.* 40 (5), 1332–1346.
- Azizkhani, M., Kadkhodapour, J., Anaraki, A.P., Hadavand, B.S., Kolahchi, R., 2020. Study of body movement monitoring utilizing nano-composite strain sensors containing Carbon nanotubes and silicone rubber. *Steel Compos. Struct.* 35 (6), 779–788. <https://doi.org/10.12989/scs.2020.35.6.779>.
- Baskoro, E.T., Haryeni, D.O., 2020. All graphs of order and diameter with partition dimension. *Heliyon*, 6.
- Brinkmann, G., Cleemput, N.V., 2011. Classification and generation of nanocones. *Discrete Appl. Math.* 159 (15), 1528–1539.
- Bultheel, A., Ori, O., 2018. Topological modeling of 1-Pentagon carbon nanocones – topological efficiency and magic sizes. *Fullerenes Nanotubes Carbon Nanostruct.* 26 (5), 291–302.
- Cataldo, F., Putz, M.V., Ursini, O., Hafez, Y., Iglesias-Groth, S., 2015. On the action of ozone on single-wall carbon nanohorns (SWCNH). *Fullerenes Nanotubes Carbon Nanostruct.* 23 (12), 1095–1102.
- Chartrand, G., Salehi, E., Zhang, P., 2000. The partition dimension of graph. *Aequationes Math.* 59, 45–54.
- Chartrand, G., Eroh, L., Johnson, M.A.O., Ortrud, R., 2000. Resolvability in graphs and the metric dimension of a graph. *Discrete Appl. Math.* 105, 99–113.
- Chu, Y.M., Nadeem, M.F., Azeem, M., Siddiqui, M.K., 2020. On sharp bounds on partition dimension of convex polytopes. *IEEE Access* 8, 224781–224790.
- Darmaji, Alfarisi, R., 2017. On the partition dimension of comb product of path and complete graph.
- Estrada-Moreno, A., 2020. On the k-partition dimension of graphs. *Theoret. Comput. Sci.* 806, 42–52.
- Faramoushjan, S.G., Jalalifar, H., Kolahchi, R., 2021. Mathematical modelling and numerical study for buckling study in concrete beams containing carbon nanotubesAdvances in Concrete Construction. 11 (6), 521–529. doi: 10.12989/acc.2021.11.6.521.
- Ge, M., Sattler, K., 1994. Observation of fullerene cones. *Chem. Phys. Lett.* 220 (3–5), 192–196.
- Hussain, Z., Kang, S.M., Rafique, M., Munir, M., Ali, U., Zahid, A., Saleem, M.S., 2019. Bounds for partition dimension of M-wheels. *Open Phys.* 17 (1), 340–344.
- Hussain, Z., Munir, M., Ahmad, A., Chaudhary, M., Khan, J.A., Ahmed, I., 2020. Metric basis and metric dimension of 1-pentagonal carbon nanocone networks. *Sci. Rep.* 10 (1).
- Iijima, S., 1991. Helical microtubules of graphitic carbon. *Nature* 354 (56).
- Iijima, S., Ichihashi, T., 1993. Single shell carbon nanotubes of one nanometer diameter. *Nature* 363, 603–605.
- Imran, M., Siddiqui, M.K., Rishi Naeem, 2018. On the metric dimension of generalized Petersen multigraphs. *IEEE Access*, 1–1.
- Johnson, M.A., 1993. Structure-activity maps for visualizing the graph variables arising in drug design. *J. Biopharm. Stat.* 3, 203–236.
- Justus, C., 2007. Boundaries of Triangle-patches and the Expander Constant of Fullerenes. *Universitat Bielefeld*.
- Khuller, S., Raghavachari, B., Rosenfeld, A., 1996. Landmarks in graphs, *Discrete Appl. Math.* 70 (3), 217–229.
- Koam, A.N.A., Ahmad, A., 2020. Barycentric subdivision of Cayley graphs with constant edge metric dimension. *IEEE Access* 8, 80624–80628.
- Koam, A.N.A., Ahmad, A., Abdelhag, M.E., Azeem, M., 2021. Metric and fault-tolerant metric dimension of hollow coronoid. *IEEE Access* 9, 81527–81534.
- Kolahchi, R., Keshtgar, B., Trung, N.-T., 2021. Optimization of dynamic properties for laminated multiphase nanocomposite sandwich conical shell in thermal and magnetic conditions. *J. Sandwich Struct. Mater.* 6. <https://doi.org/10.1177/10996362211020388>.
- Kolahchi, R., Kolahdouzan, F., 2021. A numerical method for magneto-hydro-thermal dynamic stability analysis of defective quadrilateral graphene sheets using higher order nonlocal strain gradient theory with different movable boundary conditions. *Appl. Math. Model.* 91, 458–475. <https://doi.org/10.1016/j.apm.2020.09.060>.
- Iijima, S., Ichihashi, T., Ando, Y., Pentagons, heptagons and negative curvature in graphite microtubule growth. *Nature* 356 (6372) (1992) 776–778.
- Liu, J.B., Nadeem, M.F., Azeem, M., 2020. Bounds on the partition dimension of convex polytopes. *Comb. Chem. Throughput Screening*.
- Maritz, E.C.M., Vetrik, T., 2017. The partition dimension of circulant graphs. *Quaestiones Math.* 41 (1), 49–63.
- Mehreen, N., Farooq, R., Akhter, S., 2018. On partition dimension of fullerene graphs. *AIMS Math.* 3 (3), 343–352.
- Nadeem, M.F., Azeem, M., Khalil, A., 2020. The locating number of hexagonal Möbius ladder network. *J. Appl. Math. Comput.*
- Nadeem, M.F., Azeem, M., Siddiqui, H.M.A., 2021. Comparative study of Zagreb indices for capped, semi-capped, and uncapped carbon nanotubes. *Polycyclic Aromatic Compd.*, 1–18.
- Nadeem, A., Kashif, A., Zafar, S., Zahid, Z., 2021. On 2-partition dimension of the circulant graphs. *J. Intell. Fuzzy Syst.* 40, 9493–9503.
- Saenpholphat, V., Zhang, P., 2003. Connected resolvability of graphs. *Czechoslovak Math. J.* 53 (4), 827–840.
- Sebö, A., Tannier, E., 2004. On metric generators of graphs. *Math. Oper. Res.* 29, 383–393.
- Slater, P.J., 1975. Leaves of trees. In: Proceeding of the 6th Southeastern Conference on Combinatorics, Graph Theory, and Computing, Congressus Numerantium, vol. 14, pp. 549–559.
- Valentini, F., Ciambella, E., et al, 2016. Sensor properties of pristine and functionalized carbon nanohorns. *Electroanalysis* 28 (10), 2489–2499.
- Vetrik, T., Ahmad, A., 2017. Computing the metric dimension of the categorial product of graphs. *Int. J. Comput. Math.* 94 (2), 363–371.
- Wei, C., Nadeem, M.F., Siddiqui, H.M.A., Azeem, M., Liu, J.-B., Khalil, A., 2021.. On partition dimension of some cycle-related graphs. *Math. Probl. Eng.*, 1–8